A D-band Traveling-Wave Amplifier by Embedding GaN HEMTs as Current Probes in a SiC SIW

Lei Li^{#1}, Tianze Li^{\$}, Patrick Fay^{*}, James C. M. Hwang^{\$#}

*School of Electrical and Computer Engineering, Cornell University, USA

*Department of Materials Science and Engineering, Cornell University, USA

*Department of Electrical Engineering, University of Notre Dame, USA

11886@cornell.edu

Abstract—Conventional power combiners based on coplanar or microstrip transmission lines suffer from high loss at D band or higher frequencies. By contrast, power combiners based on substrate-integrated waveguides (SIWs) can have low loss, high power capacity, and minimum crosstalk. Recently, a D-band traveling-wave amplifier (TWA) was demonstrated by embedding transistors in the middle of an SIW as voltage probes to radiate power into the SIW. The voltage probes were realized through hot through-substrate vias (TSVs), which were not supported by all semiconductor foundries. As an alternative, this work embeds transistors along the sidewalls of an SIW as current probes through standard TSVs that are grounded to the backside metal layer. This approach combines twice as many transistors per unit length of the SIW without either hot TSVs or cross-SIW interconnects. This results in at least 5-dB-higher output power compared to the previously demonstrated TWA with voltage probes. The measured output power of the present TWA at 140 GHz is at least 19 dBm, limited by the available input power. The measured output power agrees with that simulated and simulation indicates an output power of 23 dBm under 1-dB gain compression. In this proof of concept, the demonstration is based on monolithic integration of unit-cell transistors and an SIW. In the future, larger transistors in a multi-stage amplifier can be used to drive each current probe for a TWA of higher gain, output power, and efficiency. The present concept of efficient power combining is equally applicable to heterogeneous integration and is material- and technology-agnostic. For example, transistors can be fabricated in a Si chiplet before integration with an SIW fabricated in a Si interposer.

Keywords— millimeter wave, MMICs, power amplifiers, power combiners, substrate integrated waveguides.

I. INTRODUCTION

With the operating frequencies of 6G wireless communications and next-generation automotive radars extending above 110 GHz, D-band (110–170 GHz) high-power transmitters are needed [1]–[3]. However, conventional microwave monolithic integrated circuits (MMICs) based on coplanar or microstrip transmission lines suffer from high loss, significant crosstalk, and limited power capacity above 110 GHz. For example, the output power of D-band MMICs is presently limited to the order of 20 dBm by not only the speed of transistors, but also the loss of power combiners [4]. In particular, the loss of conventional power combiners increases significantly with the number of interconnected transistors, resulting in diminishing returns for combining more transistors. By contrast, substrate-integrated waveguides (SIWs) [5] have

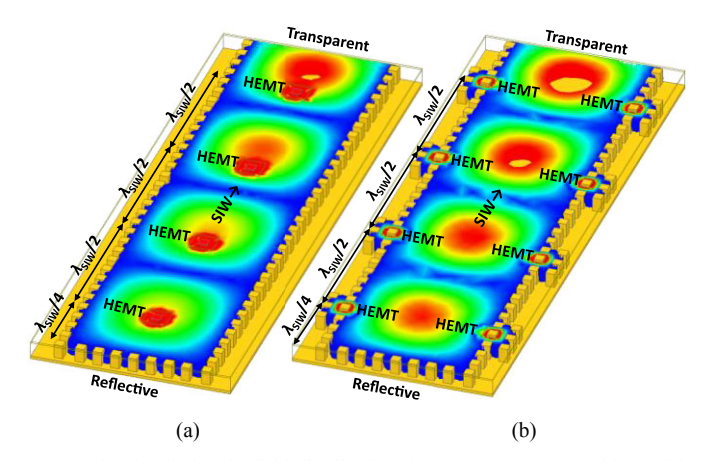


Fig. 1. Simulated electric field distributions in an SIW power combiner with HEMTs as (a) voltage probes and (b) current probes to radiate power into the SIW. Color scale indicates field magnitude, the redder, the higher.

low loss, minimal crosstalk, and high power capacity. However, because the size of an SIW is on the order of the guided wavelength λ_{SIW} in the SIW, SIWs are usually implemented at the board level.

SIW-based monolithic integration becomes feasible when the frequency exceeds 110 GHz, so that $\lambda_{SIW} \leq 1$ mm in typical semiconductors such as Si, SiC, GaAs, GaN and InP [6]. Although SIW combiners have been demonstrated in corporate, serial, radial, Wilkinson, and Gysel structures at the board level [7], these structures when scaled to the D band are still too large for monolithic integration. At the D-band, compact SIW combiners can only be realized by embedding transistors in the SIW. For example, recently, a 14-dBm D-band traveling-wave amplifier (TWA) was reported by embedding transistors in the middle of an SIW as voltage probes to radiate power into the SIW [Fig. 1(a)] [8], [9]. The voltage probes were realized through hot through-substrate vias (TSVs), which were not supported by all semiconductor foundries. This paper reports a > 19-dBm D-band TWA by embedding transistors along the sidewalls of an SIW as current probes through standard TSVs that are grounded to the backside metal layer [Fig. 1(a)]. Compare to [8], [9], the present TWA combines twice as many transistors in an SIW of the same length without either hot TSVs or cross-SIW interconnects. Note that the TE_{10} wave in an SIW has voltage peaks in the middle and current peaks on the sidewalls.

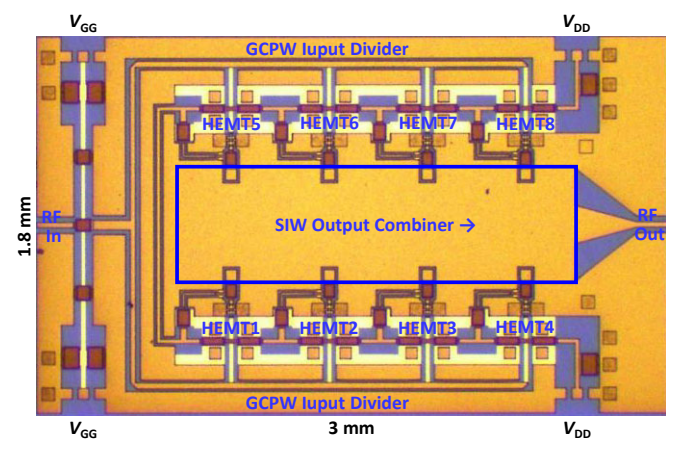


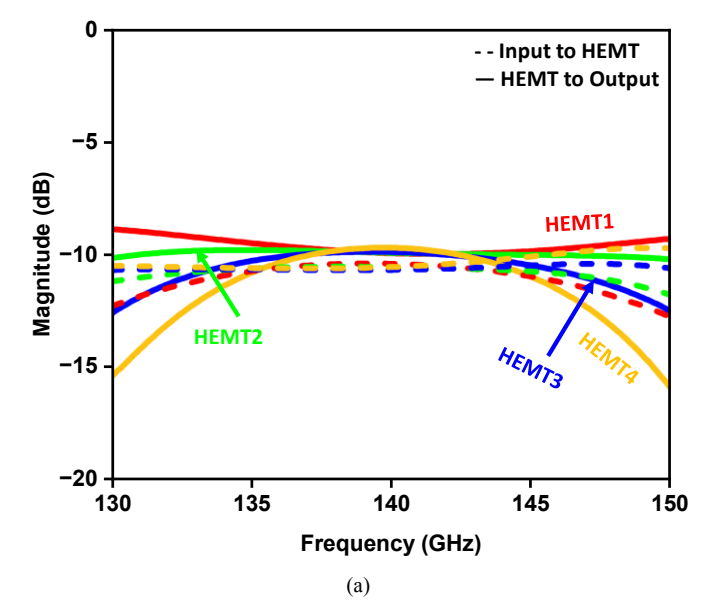
Fig. 2. Micrograph of a TWA chip.

For high-power MMICs based on GaN-on-SiC highelectron-mobility transistors (HEMTs), SIW combiners are especially attractive because the HEMTs can be monolithically integrated with a SiC SIW without additional process complexity. SiC is an excellent SIW material, because it offers a high dielectric constant for compact size, high electrical resistivity and low loss tangent for low loss, high breakdown strength for high power capacity, strong mechanical toughness for robust fabrication, and high thermal conductivity for heat dissipation [10].

II. DESIGN

The present TWA is designed and fabricated in HRL's T3 40-nm GaN-on-SiC HEMT technology with cutoff frequencies $f_{\rm T} \sim 200$ GHz and $f_{\rm MAX} \sim 400$ GHz [11]. The SiC substrate is 50-μm thick. As shown in Fig. 2, the TWA has an input divider made of a grounded coplanar waveguide (GCPW) and an output combiner made of an SIW. The divider consists of two primary branches, with each primary branch consisting of four secondary branches. The divider delivers the input signal to each HEMT evenly in magnitude but delayed by 180° between adjacent HEMTs on each side of the SIW. Broadband phase synchronization between the divider and the combiner is challenging because quasi-transverse-electromagnetic (*TEM*) waves travel in the GCPW whereas transverse-electric (TE) waves travel in the SIW, the latter being more dispersive [12]. Nevertheless, the GCPW and the SIW can be designed so that their phase velocities match at a single frequency of 140 GHz. Specifically, the GCPW is 30-µm wide with a characteristic impedance $Z_0 = 37 \Omega$ and a wavelength $\lambda_{GCPW} = \lambda_{SIW} = 900 \mu m$ at 140 GHz. The SIW is bound by two TSV rows 540- μ m apart center-to-center with a cutoff frequency of 90 GHz. Each TSV has a 30 μ m × 30 μ m cross section. The left end of the SIW is terminated in a row of TSVs after $\lambda_{SIW}/4$. The right end of the SIW is transitioned to GCPW to facilitate wafer probing with an extra loss of 0.2 dB [6]. The HEMTs are lined along each SIW sidewall in a period of $\lambda_{SIW}/2$.

Fig. 3 shows HFSS-simulated magnitudes and phases of the divider and combiner. At 140 GHz, the magnitude of the transmission coefficient from the GCPW input to each HEMT is -10.6 dB, whereas the magnitude of the transmission



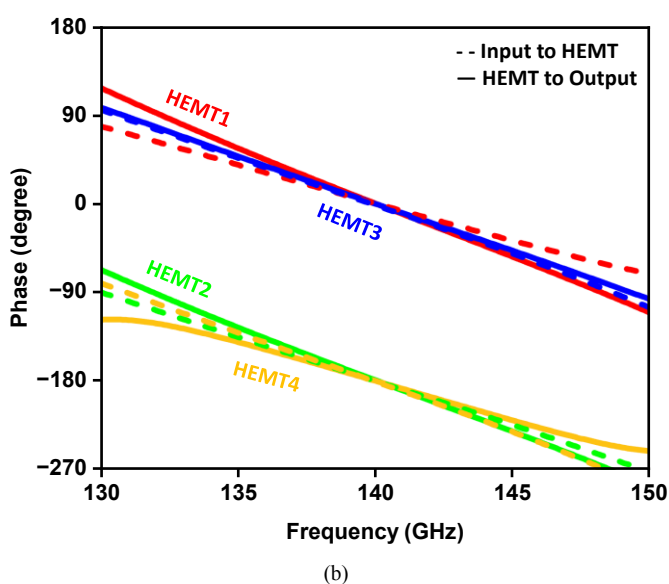
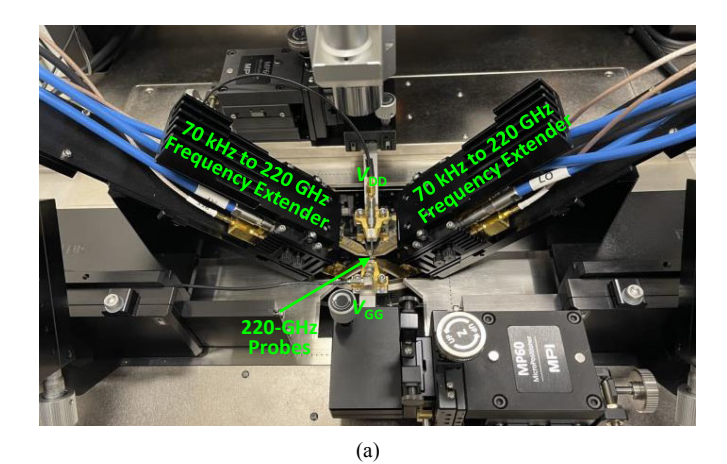


Fig. 3. HFSS-simulated (a) magnitudes and (b) phases of the transmission coefficients of the GCPW input to each HEMT and from each HEMT to the SIW output.

coefficient from each HEMT to the SIW output is -9.7 dB. Considering the transmission coefficient of an ideal 8-way divider or combiner is -9 dB, the present divider/combiner is 70%/86% efficient with 1.6 dB/0.7 dB extra loss. This confirms that the SIW combiner is significantly better than D-band on-chip combiners based on coplanar or microstrip transmission lines [6]. Considering the SIW is $2\lambda_{\text{SIW}}$ long, the 0.7-dB loss of the SIW combiner is consistent with the 0.3-dB/mm loss previously reported for the same technology at the D band [8], [9]. Note the technology can be improved because the SIW loss is presently limited by metal loss instead of dielectric or radiation loss [13], [14]. Fig. 3(b) confirms that input and output phases are synchronized around 140 GHz, with adjacent HEMTs differing by 180° as intended.



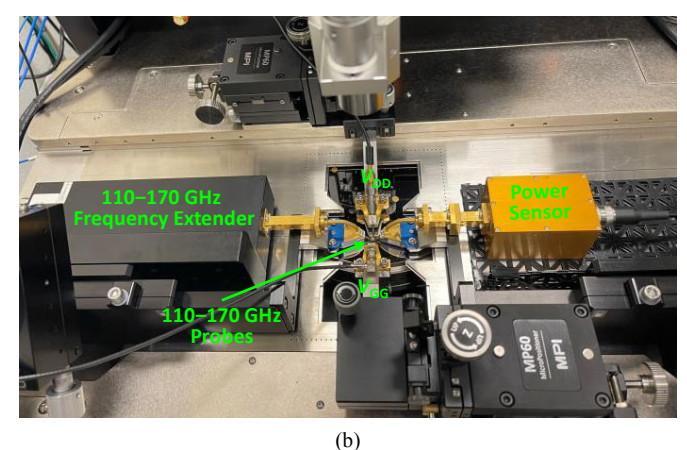


Fig. 4. (a) Small- and (b) large-signal measurement setups.

The input and output impedances of each $2 \times 25~\mu m$ HEMT are optimized through source- and load-pull simulations using HRL's HEMT model. Under a class-AB gate bias of $V_{\rm GG} = -0.1~\rm V$, a drain bias of $V_{\rm DD} = 12~\rm V$, and an input power $P_{\rm IN} = 5.7~\rm dBm$ at 140 GHz and (14.4 + j3.8) Ω , each HEMT can supply an output power $P_{\rm OUT} = 10.2~\rm dBm$ and a gain of 4.5 dB to a current probe with an optimum load impedance of (25 + j60) Ω . The load impedance of each current probe is adjusted by the TSV's position and gap in the top ground plane.

III. MEASUREMENT

Small-signal characteristics of the fabricated TWA are measured from 120 to 160 GHz using an Anritsu ME7838G vector network analyzer, two Anritsu MA25400A frequency extenders, and two MPI TITAN T220A-GSG050 probes [Fig. 4(a)] [15]. The measured scattering parameters are deembedded to the probe tips by using the load-reflect-reflect-match method [16] and an MPI TCS-050-100-W impedance standard substrate. Large-signal characteristics are measured from 130 to 150 GHz by replacing the input frequency extender with a VDI WR6.5VNATxRxM frequency extender, the output frequency extender with an Erickson PM5B power meter, and the probes with FormFactor I170-S-GSG-50-BT waveguide probes [Fig. 4(b)]. With an input power from 0 to 16 dBm, large-signal characteristics are calibrated to the probe tips through a low-loss through line [17].

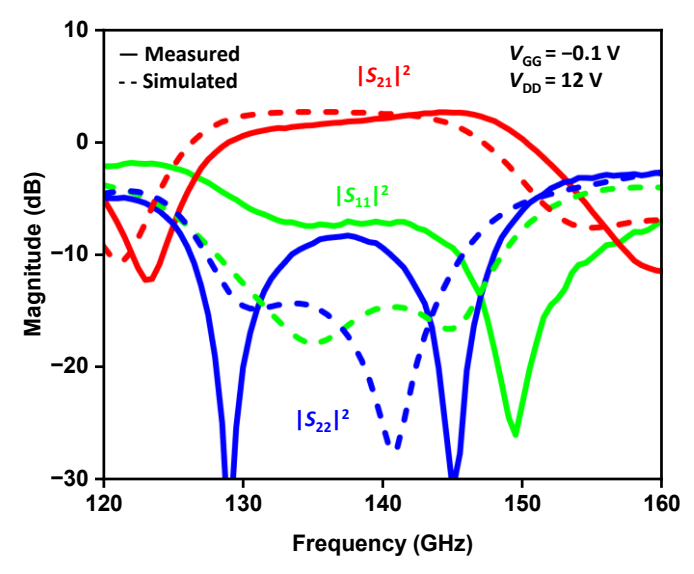


Fig. 5. Measured vs. simulated small-signal characteristics of a TWA.

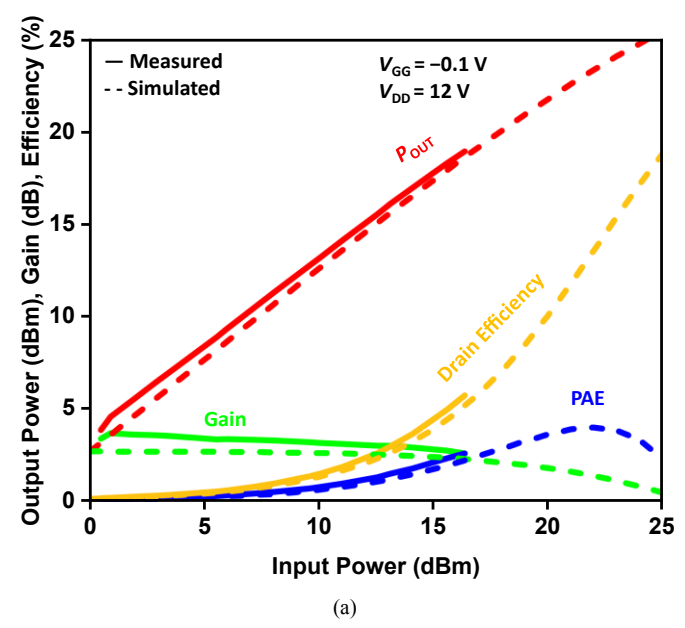
IV. RESULTS

Fig. 5 shows the small-signal scattering parameters from 120 to 160 GHz of a TWA. In general, the measured result agrees with that simulated except for moderate blue shifts and somewhat higher reflections. The peak gain is 2.6 dB with a 3-dB bandwidth of 128–150 GHz. The difference between the simulated HEMT gain of 4.5 dB and the measured TWA gain of 2.6 dB is consistent with the simulated total loss of the divider and combiner 1.6 dB + 0.7 dB \approx 2 dB. The blue shifts could be due to the foundry-specified dielectric constant of SiC used in the design. By using the method in [13], [14] to characterize the dielectric constant, better agreement could be achieved. The higher reflection could be due to imprecise modeling of the passive components.

Fig. 6(a) shows $P_{\rm OUT}$ vs. $P_{\rm IN}$ of a TWA at 140 GHz. It can be seen that the measured characteristics agree with that simulated except that the measured $P_{\rm OUT}$ stops at 19 dBm as limited by the maximum available $P_{\rm IN}$ of 16 dBm. Meanwhile, the simulated $P_{\rm OUT}$ continues to increase with increasing $P_{\rm IN}$ suggesting a $P_{\rm OUT}$ of 23 dBm under 1-dB gain compression. Fig. 6(b) shows $P_{\rm OUT}$, drain efficiency, and power-added efficiency (PAE) as a function of frequency under a constant $P_{\rm IN}$ of 16 dBm. It can be seen that the large-signal bandwidth agrees with the small-signal bandwidth.

V. CONCLUSION

The above results provide the proof of concept that, at D band, transistors can be embedded along the sidewalls of an SIW as current probes for efficient power combining. Compared to the previous demonstrations of embedding transistors in the middle of an SIW as voltage probes, the present TWA can combine twice as many transistors per unit length of the SIW without hot TSVs or cross-SIW interconnects. The result is > 19 dBm output power vs. the previously reported 14 dBm output power. Because presently the output power is limited by the available input power, in the future larger



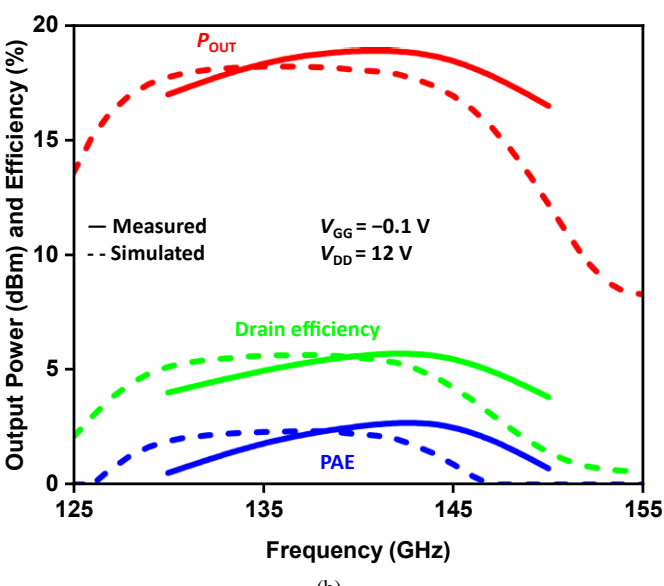


Fig. 6. Measured vs. simulated large-signal characteristics as a function of (a) input power and (b) frequency.

transistors in a multi-stage amplifier [18] can be used to drive each current probe to realize a TWA of higher gain, output power, and efficiency.

For proof of concept, the present demonstrating is based on monolithic integration of transistors with an SIW. The concept is equally applicable to heterogeneous integration and is material- and technology-agnostic. For example, transistors can be fabricated in a Si chiplet before integration with an SIW fabricated in a Si interposer.

ACKNOWLEDGMENT

This work is supported in part by the US National Science Foundation (NSF) under Grants ECCS-2117305, ECCS-2122323 and ECCS-2132329, the US Army Research Office under Grant W911NF2410023, the US Department of Defense under the State of the Art Radio Frequency Gallium Nitride program, and the Semiconductor Research Corporation and the US Defense Advanced Research Projects Agency through the Joint University Microelectronics Program.

REFERENCES

- [1] W. Hong *et al.*, "The role of millimeter-wave technologies in 5G/6G wireless communications," *IEEE J. Microw.*, vol. 1, no. 1, pp. 101–122, Jan 2021
- [2] C. Waldschmidt, J. Hasch, and W. Menzel, "Automotive radar—From first efforts to future systems," *IEEE J. Microw.*, vol. 1, no. 1, pp. 135– 148, Jan. 2021.
- [3] T. Maiwald *et al.*, "A review of integrated systems and components for 6G wireless communication in the D-band," *Proc. IEEE*, vol. 111, no. 3, pp. 220–256, Mar. 2023.
- [4] H. Wang *et al*, "Power amplifiers performance survey 2000-present," [Online]. Available: https://ideas.ethz.ch/Surveys/pa-survey.html.
 [5] K. Wu, M. Bozzi, and N. J. G. Fonseca, "Substrate integrated
- [5] K. Wu, M. Bozzi, and N. J. G. Fonseca, "Substrate integrated transmission lines: Review and applications," *IEEE J. Microw.*, vol. 1, no. 1, pp. 345–363, Jan. 2021.
- [6] M. J. Asadi et al., "Substrate-integrated waveguides for monolithic integrated circuits above 110 GHz," in *IEEE MTT-S Int. Microw. Symp. Dig.*, Atlanta, GA, USA, Jun. 2021, pp. 669–672.
- [7] S. H. Shehab, N. C. Karmakar, and J. Walker, "Substrate-integrated-waveguide power dividers: An overview of the current technology," *IEEE Antennas Propag. Mag.*, vol. 62, no. 4, pp. 27–38, Aug. 2020.
- [8] L. Li, T. Li, P. Fay, and J. C. M. Hwang, "A D-band frequency-doubling distributed amplifier through monolithic integration of SiC SIW and GaN HEMTs," in *Asia-Pacific Microw. Conf. (APMC)*, Taipei, Taiwan, Dec. 2023, pp. 1–3.
- [9] L. Li, P. Fay, and J. C. M. Hwang, "A D-band frequency-doubling solidstate traveling-wave amplifier through monolithic integration of a SiC SIW and GaN HEMTs." Submitted to *IEEE J. Microw*.
- [10] G. L. Harris, Properties of Silicon Carbide, London, UK: INSPEC, 1995.
- [11] K. Shinohara et al., "Scaling of GaN HEMTs and Schottky diodes for submillimeter-wave MMIC applications," *IEEE Trans. Electron Devices*, vol. 60, no. 10, pp. 2982–2996, Oct. 2013.
- [12] D. M. Pozar, Microwave Engineering, 4th ed, New York, NY, USA: Wiley, 2011.
- [13] L. Li et al., "Extraordinary permittivity characterization using 4H-SiC substrate-integrated waveguide resonators," in 100th ARFTG Microw. Meas. Symp., Las Vegas, NV, USA, Jan. 2023, pp. 1–4.
- [14] L. Li, S. Reyes, M. Javad Asadi, P. Fay, and J. C. M. Hwang, "Extraordinary permittivity characterization of 4H SiC at millimeterwave frequencies," *Appl. Phys. Lett.*, vol. 123, no. 1, p. 012105, Jul. 2023.
- [15] L. Li, S. Reyes, M. J. Asadi, W. D. Jena, H. G. Xing, P. Fay, and J. C. M. Hwang, "Single-sweep vs. banded characterizations of a D-band ultra-low-loss SiC substrate integrated waveguide" in 99th ARFTG Microw. Conf., Denver, CO, USA, Jun. 2022, pp. 75–78.
- [16] A. Davidson, K. Jones, and E. Strid, "LRM and LRRM calibrations with automatic determination of load inductance," in 36th ARFTG Conf. Dig., Monterrey, CA, USA, Nov. 1990, pp. 57–63.
- [17] T. Li, L. Li, and J. C. M. Hwang, "Validity of room-temperature calibration for on-wafer measurements up to 220 GHz, 125 °C, and 48 h," in *ARFTG Microw. Conf.*, San Diego, CA, USA, Jun. 2023, pp. 1–4.
- [18] M. Cwiklinski et al., "D-band and G-band high-performance GaN power amplifier MMICs," *IEEE Trans. Microw. Theory Techn.*, vol. 67, no. 12, pp. 5080-5089, Dec. 2019.